Transition in Tethered Layer Thickness Induced by Concentration Changes in a Spread Film of an Amphiphilic Graft Copolymer

Aline F. Miller and Randal W. Richards*

Interdisciplinary Research Centre in Polymer Science and Technology, University of Durham, Durham DH1 3LE, UK

John R. P. Webster

ISIS Science Division, Rutherford Appleton Laboratory, Chilton, Didcot, Oxon OX 11 0QZ, UK

Received May 21, 2001; Revised Manuscript Received August 21, 2001

ABSTRACT: Three well-defined graft copolymers and a polynorbornene backbone with a poly(ethylene oxide) graft on each backbone repeat unit have been synthesized with fully hydrogenous and deuterated poly(ethylene oxide) grafts. The graft copolymers have a backbone degree of polymerization of 50 and the degrees of polymerization of the poly(ethylene oxide) grafts in the separate copolymers have values of 15, 25, and 50. Each of these copolymers has been spread at the air−water interface as Langmuir films with surface concentrations from 0.3 to 4.0 mg m^{-2}. The spatial extent of the regions occupied by the backbone and the grafts has been determined by neutron reflectometry. The polynorbornene backbone is confined to the air phase and contains an appreciable amount of air, the volume fraction of which increases as the surface concentration of graft copolymer increases. The poly(ethylene oxide) grafts are essentially totally immersed in the aqueous subphase, the distribution of ethylene oxide segments being described by a combination of a uniform layer with a parabolic tail. This description applies for all surface concentrations. The total thickness of the poly(ethylene oxide) layer increases with surface concentration in manner that is very similar to that predicted by single-chain mean-field theory for brushlike layers formed by block copolymers where there is a repulsive interaction between the tethered blocks and the anchor blocks. At the highest surface concentration the layer thickness is ca. 3−5 times the radius of gyration of the poly(ethylene oxide) grafts. There is no evidence for a first-order transition in the layer thickness at a critical surface concentration of the graft copolymers. Individual thicknesses of the uniform layer and parabolic regions show quite different behavior. The parabolic region thickness approaches an asymptotic value at high surface concentrations. The uniform layer thickness at first shows no change in layer thickness as surface concentration increases but then begins to increase abruptly at a surface concentration that increases as the degree of polymerization of the poly(ethylene oxide) grafts decreases.

Introduction

Some 25 years ago a seminal paper by Alexander[1] introduced the notion of tethered polymers and outlined their properties, notably the relation between the thickness or height of the tethered molecules and the number of polymer molecules per unit area, the grafting density, when surrounded by a thermodynamically favorable solvent above the tethering surface. Since the original description there have been modifications and reexaminations,[2−6] but the basic idea of the stretching of the chains at high grafting densities to form a brushlike layer of polymer molecules has remained central to all subsequent revisions.

Tethered polymer layers play a key role in many applications, e.g., stabilization of colloidal dispersions,[7] self-assembly at solid surfaces, inhibition of deposition on to surfaces,[8] and the intrinsic stabilization of copolymer micelles.[9] The theoretical descriptions of tethered polymer layers have been accompanied by experimental investigations on a wide variety of tethered polymer systems: thin films of polymer melts on solid substrates,[10] polymers grafted to porous substrates and particulate surfaces,[11] and polymers adsorbed or spread on fluid surfaces.[12−15] A variety of techniques have been used: quasi-elastic light scattering,[16] small-angle neutron scattering,[11,17] force−distance curves,[18] and both X-ray and neutron reflectometry.[13−15,19−23] The latter probably providing the most direct data for the distribution of polymer normal to the tethering surface. Where polymers are grafted to a solid surface there is generally little control over the extent of grafting; for adsorption at solid surfaces from solution, the molecules adsorbed at early times may prevent adsorption at longer times, and thus the grafting density may not become sufficiently high to be in the grafted brush regime.

In principle, spreading an amphiphilic copolymer at the surface of a fluid enables control of the grafting density. The presumption is that the fluid phase is an infinitely poor solvent for one copolymer component and resides at the surface, acting therefore as an anchor for the other component that is solvated by the liquid subphase. Subsequent compression of the Langmuir film increases the grafting density in a known way. Much of the experimental work on such spread amphiphilic copolymer films has used aqueous subphases. Consequently, the high surface energy has meant that the solvated polymer layer usually has rather modest dimensions and does not extend deeply into the subphase. One exception to this is the polydimethylsiloxane−polystyrene diblock copolymer spread at the surface of ethyl benzoate, a nonsolvent for the siloxane block but a good solvent for the polystyrene block, for which both surface pressure and neutron reflectometry results have been discussed.[24−31] The polystyrene blocks extend into the organic subphase on compression; but the finite area occupied by the insoluble blocks limits the grafting densities attainable, and even at the highest surface concentrations the grafting density may

10.1021/ma010873t CCC: $20.00
Published on Web 10/04/2001

pertain to some intermediate state rather than conform strictly to that for a brush layer.

We report here the organization of an amphiphilic graft copolymer (polynorbornene backbone with poly(ethylene oxide) grafts) spread at the air−water interface. The architecture of the graft copolymer is such that the grafting density along the chain is high. The distribution of the poly(ethylene oxide) (PEO) grafts normal to the surface has been obtained by neutron reflectometry, and we begin by summarizing pertinent background theory for tethered chains surrounded by good solvent.

Theoretical Background

A major difference between the scaling law description of a polymer brush layer and the analytical self-consistent-field theory is the location of the free chain ends. In the latter these are located throughout the layer thickness while the simpler scaling theory places them all at the same distance, the brush height, h, from the tethering surface. Both lead to the same scaling exponent in the relation between brush height and grafting density, σ. For the self-consistent-field theory

$$h = \left(\frac{\pi^2}{72pv}\right)^{-1/3} Na^{5/3}\sigma^{1/3} \tag{1}$$

where v is the excluded-volume parameter and p the stiffness parameter of the tethered molecule. The volume fraction distribution normal to the surface has a parabolic distribution given by

$$\phi(z) = \frac{3\bar{\phi}}{2}(1 - z^2/h^2) \tag{2}$$

where z is the distance normal to the surface and $\bar{\phi}$ is the average volume fraction of polymer in the brush layer given by

$$\bar{\phi} = \frac{\sigma N}{h}\, a^3 \tag{3}$$

N being the degree of polymerization of the brush forming polymer with a statistical step length, a.

A feature of the initial theory[1] was the prediction of a first-order transition from a "pancake" to a brush configuration for tethered chains that have attractive interactions with the tethering surface. Ligoure[32] has also predicted such a first-order phase transition, but as yet there has been no direct evidence for their occurrence. The density distribution of grafted poly(ethylene oxide) chains has recently been simulated by Monte Carlo methods.[33] No first-order transition was noted in the average brush height as the effective grafting density increased, and the density profile was parabolic, the brush height, h, scaling with the grafting density with an exponent that was close to $^1/_3$ in good solvent conditions.

Szleifer[34−37] has applied a single-chain mean-field theory to an A−B copolymer at a fluid surface where the B block lies on the surface, and there are repulsive interactions between these and the solvated A blocks. The total repulsion will thus depend on the surface coverage by the B blocks since the repulsion is quantified by an interaction parameter, χ_{rep}, per A−B monomer interaction. When $\chi_{rep} = 0$, the surface pressure−area isotherm exhibits a plateau at rather low areas per molecule. As the magnitude of χ_{rep} increases, i.e., more unfavorable interactions, this plateau transforms to a van der Waals loop, the appearance of which is a symptom of a first-order phase transition. Associated with these observations on the behavior of the surface pressure is a parallel calculation of the polymer layer thickness. At low grafting densities there is no change in the layer thickness, which is considerably smaller than the radius of gyration of the grafted polymer, i.e., a pancake configuration; at the transition there is a rapid increase in the thickness due to the A−B repulsions and excluded-volume interactions between the A chains. Figure 1 shows schematically the surface pressure and brush height variation with surface coverage obtained by Szleifer for small and large values of χ_{rep}. For low values of χ_{rep} the brush height, h, is anticipated to change smoothly with increasing grafting density σ, and the composition distribution normal to the surface is postulated to have a large magnitude near the surface, decaying to a brushlike structure deeper into the fluid subphase. When the repulsive interactions are larger, the layer thickness increases very rapidly over a small range of surface concentrations and then exhibits a weaker dependence on the number density of end-tethered molecules at the air−liquid subphase interface.

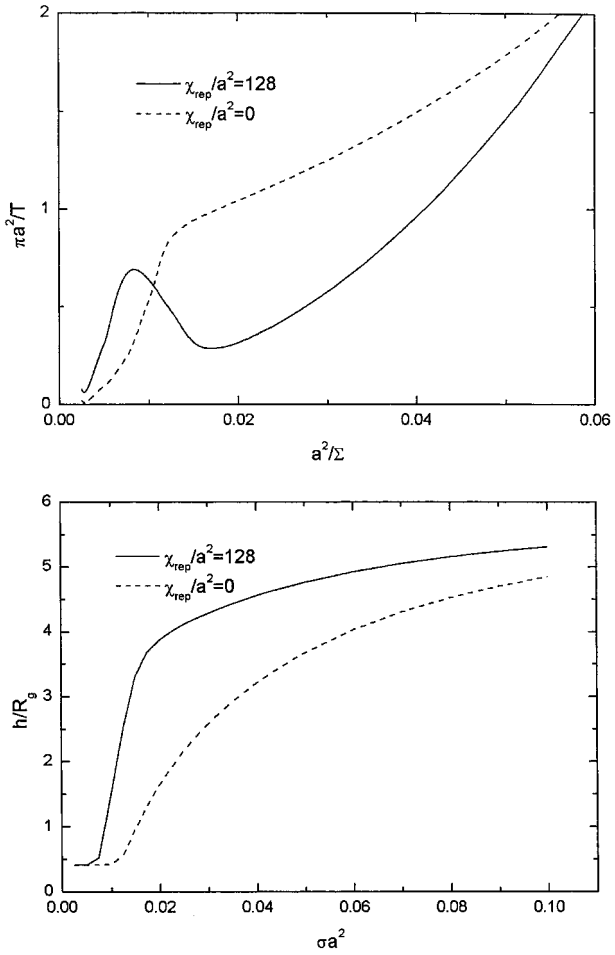

Figure 1. Surface pressure (a) and tethered layer height (b) dependence on normalized grafting density from single-chain mean-field theory for repulsion energies of zero and very large.

Experimental Section

Graft Copolymers. The synthesis of the graft copolymers by a combination of anionic and ring-opening polymerization methods has been set out in detail in an earlier publication.[22]

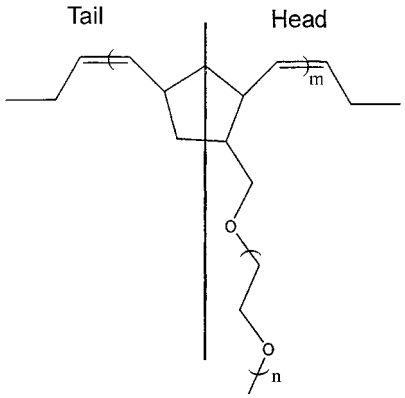

Figure 2. Schematic of the structure of graft copolymer repeat unit.

Table 1. Macromer and Graft Copolymer Molecular Weights and Radius of Gyration of Poly(ethylene oxide) Grafts

copolymer	isotopic nature of PEO	$\bar{M}_w$/g mol^{-1} macromer	$\bar{M}_w$/g mol^{-1} copolymer	R_g/Å of PEO graft
n15	H	1052	52 600	11
n15	D	965	48 250	11
n25	H	1480	74 000	14
n25	D	1590	79 500	15
n50	H	2292	114 600	18
n50	D	2702	135 100	20

Figure 2 shows the schematic structure of the copolymer and polymerization conditions were chosen such that the polynorbornene backbone had a degree of polymerization, m, of 50. Three copolymers were prepared, the degree of polymerization (n) of the poly(ethylene oxide) grafts of each being 15, 25, and 50. A series of copolymers were also made with deuteriopoly(ethylene oxide) grafts, the molecular weights being similar to those of the hydrogenous copolymers. Table 1 gives the molecular weights of the macromer precursor and the graft copolymers obtained by size exclusion chromatography. The n15 copolymer was shown by ^{1}H NMR to have a backbone tacticity that was equally cis and trans whereas the n25 and n50 copolymers had tacticities that were 33% cis and 67% trans. Furthermore, the NMR spectra also showed macromer addition to the growing chains was mainly tail−head for cis addition and tail−tail for the trans arrangements of backbone repeat units. In Figure 2 we have indicated the head and tail regions of the repeat unit, these being purely arbitrary and are identification purposes only.

Surface Pressure Isotherms. A NIMA (Coventry, UK) model 2001 Langmuir film balance was used to obtain surface pressure isotherms at 298 K, the trough being placed on an active vibration isolation table. The usual procedure was to deposit 20 μL of a 1.0 mg mL^{-1} chloroform solution of each copolymer on to the freshly aspirated surface of high-purity water (18 MΩ cm) and the spread film allowed to stand for 20 min to permit solvent evaporation. The film was then compressed at a rate of 30 cm^2 min^{-1} from an initial area of 900 to 80 cm^2, the surface pressure being recorded continuously.

Neutron Reflectometry. Neutron reflectometry data were obtained using the CRISP and SURF reflectometers at the UK pulsed neutron source, ISIS, located at the Rutherford Appleton Laboratory, Didcot, UK. A rectangular NIMA trough was mounted in the neutron beam and enclosed by a box with quartz inlet and outlet windows for incident and specularly reflected neutron beams. The purpose of the enclosure was to reduce exchange between heavy water used in the subphase and atmospheric moisture. The momentum transfer perpendicular to the surface was $0.02 \leq Q/\text{Å}^{-1} \leq 0.6$, and the reflectivity values were placed on an absolute scale using calibration factors obtained from the reflectivity of a clean D_2O subphase.

The spread film−aqueous subphase combinations used were part deuterated (i.e., the PEO grafts) copolymer on heavy water and part deuterated copolymer on null reflecting water (nrw), i.e., that combination of light and heavy water that has a net scattering length density of zero.

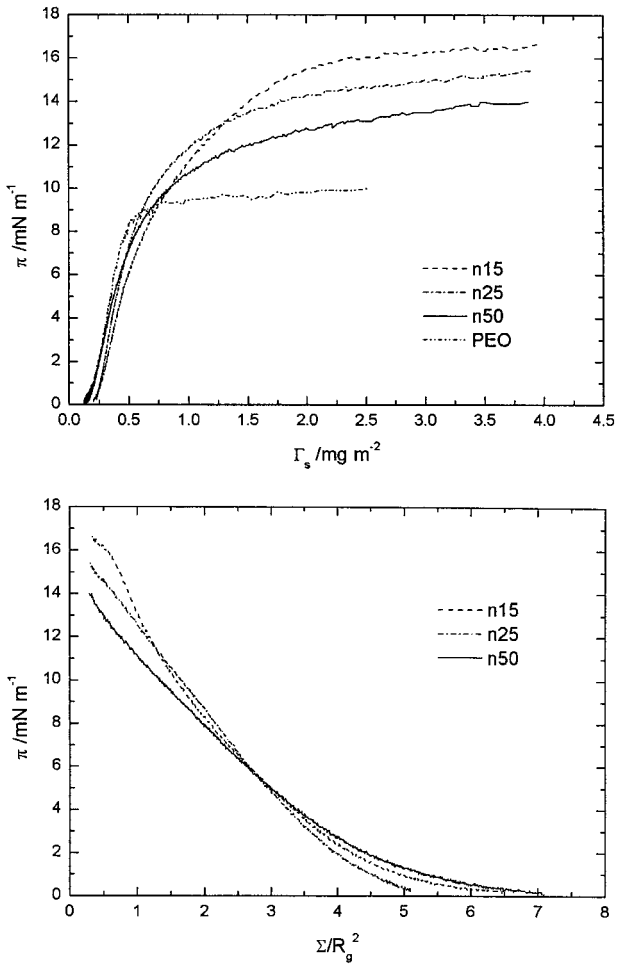

Figure 3. Surface pressure isotherms for all graft copolymers (a) as a function of surface concentration and (b) as a function of area per PEO graft normalized by the square of the radius of gyration.

Results

Surface Pressure Isotherms. For each of the hydrogenous graft copolymers, the surface pressure isotherm is shown in Figure 3. At low surface concentrations the graft copolymers have rather similar values of surface pressure at the same surface concentrations. Differences become apparent at surface concentrations greater than ca. 1.5 mg m^{-2}. The n50 copolymer has the lower surface pressure of the three, and the n15 copolymer has the highest value over the range $1.5 \leq \Gamma_s/\text{mg m}^{-2} \leq 4$. All the isotherms have approximately similar shapes, but for the n15 copolymer the surface concentration at which plateau values are approached is much higher being ca. 2 mg m^{-2} compared to approximately 1.5 mg m^{-2} for the n50 and n25 graft copolymers. Qualitatively, these values can be interpreted as a greater desorption of some (or all) of the n50 graft copolymer from the air−water interface. For comparison with the predictions of Szleifer[35,36] and isotherms from the analytical self-consistent-field theory, surface pressures are plotted as a function of normalized area per graft (Σ/R_g^2) in Figure 3b. None of the curves exhibit any evidence of a van der Waals loop, and only the isotherm for the n15 copolymer shows a feature that

may be attributable to plateau formation heralding a transition from a "pancake" configuration to a more extended layer structure at very low values of Σ/R_g^2, i.e., approaching a surface concentration of 4.0 mg m^{-2}.

NMR analysis shows that the copolymers are between 83% (n15) and 96% (n50) by weight poly(ethylene oxide), and thus we have applied the scaling relation between surface pressure and surface concentration to obtain the exponent and gain some insight into the nature of the thermodynamic interactions. The scaling relation is[38−40]

$$\pi \sim \Gamma_s^{\,y} \tag{4}$$

where $y = 2\nu/(2\nu - 1)$, ν being the Flory swelling exponent describing the scaling between polymer dimensions and degree of polymerization.

Double-logarithmic plots of surface pressure as a function of surface concentration were distinctly more curved than for homopoly(ethylene oxide) spread films at the air−water interface; however there was a limited range of Γ_s to which linear fits can be obtained (0.1−0.25 mg m^{-2}) and thus values of ν obtained. As n increased from 15 to 50, the three values of ν obtained were 0.62, 0.64, and 0.68. Over a larger range of Γ_s (to 0.4 mg m^{-2}) the equivalent procedure applied to the surface pressure data for a spread film of PEO homopolymer gives a value of ν equal to 0.71, i.e., very close to the value of 0.75 predicted when the thermodynamic interactions between polymer and subphase are favorable. For the graft copolymers, increasing the PEO content makes polymer−aqueous subphase interactions more favorable, but evidently there are distinct differences between spread films of poly(ethylene oxide) and the graft copolymers as a comparison of the isotherms shows (Figure 3).

Neutron Reflectometry. Figure 4 shows the neutron reflectometry profiles for the n15 copolymer with deuterated grafts at selected surface concentrations spread on an nrw subphase. The anticipated increase in reflectivity is observed as the surface concentration increases and more deuterated material is present at the surface, increasing the scattering length density. For $\Gamma_s \geq 2.0$ mg m^{-2}, there is almost negligible change in the reflectivity profiles apparent to the eye. Reflectivity profiles for the n15 and n50 graft copolymers at the highest and a lower film concentration are shown in Figure 4b,c. At a high surface concentration, the n50 copolymer has a slightly lower reflectivity than the n15 copolymer despite having the largest content of deuterated PEO. This suggests that there is less PEO near the air−water interface; i.e., the grafts are extending to greater depths into the subphase. At low surface concentrations the reflectivity from the n50 spread film has a distinctly different curvature compared to that of the n15 graft copolymer and suggests a rather different near-surface arrangement of the PEO grafts in this copolymer.

An exhaustive discussion of the analysis of neutron reflectivity data, the models used, and a comparison of their accuracy in predicting the surface concentration of the spread copolymer has been given in our earlier paper. In the earlier paper we discussed only a limited range of surface concentrations for the n25 copolymer. The model for the distribution of copolymer at the air−water interface that provided the best agreement with the known spread concentration consisted of a uniform layer of polynorbornene containing no water on the

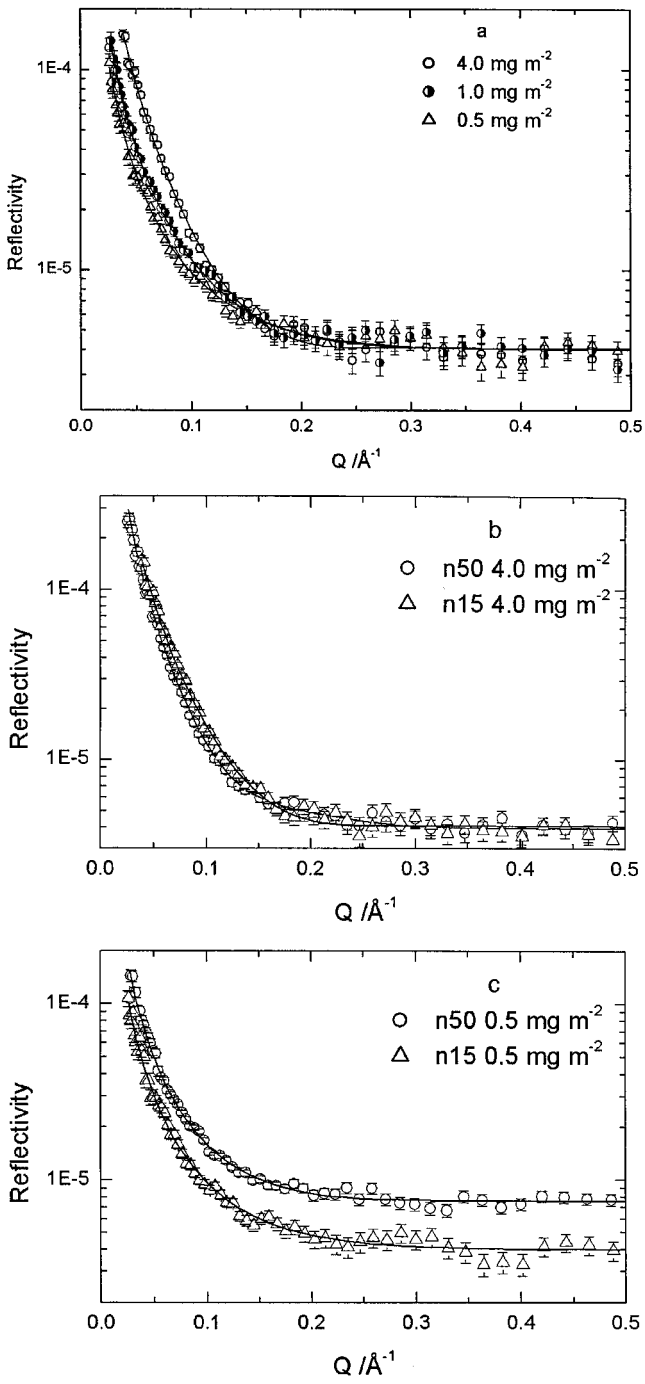

Figure 4. (a) Reflectivity profiles for the n15 copolymer with deuterated poly(ethylene oxide) grafts spread on null reflecting water at the surface concentrations indicated. (b) Reflectivity profiles for the n50 and n15 copolymers at $\Gamma_s = 4.0$ mg m^{-2} and (c) at $\Gamma_s = 0.5$ mg m^{-2}. The different backgrounds evident in (c) arise from the different backgrounds intrinsic to the CRISP and SURF reflectometers. The lines through the data points are the best nonlinear least-squares fit to the data using the uniform layer−parabola model shown schematically in Figure 5.

water surface. The poly(ethylene oxide) grafts were essentially completely immersed in the aqueous subphase and distributed as a uniform layer immediately below the surface with a parabolic tail for the regions of the layer furthest from the air−water interface. This model has been used to analyze all the neutron reflectivity data discussed here. A number density distribution of copolymer segments is shown schematically in Figure 5, which also indicates the various parameters

Table 2. Polynorbornene Backbone Layer Thickness and Volume Fraction Composition

	n15			n25			n50		
Γ/mg m^{-2}	d/Å	ϕ_{polym}	ϕ_{air}	d/Å	ϕ_{polym}	ϕ_{air}	d/Å	ϕ_{polym}	ϕ_{air}
4.0	4 ± 2	0.37	0.6	5 ± 2	0.26	0.74	5 ± 2	0.6	0.33
3.5	4 ± 2	0.34	0.58	6 ± 1	0.22	0.78	5 ± 1	0.3	0.63
3.0	5 ± 2	0.28	0.66	5 ± 1	0.27	0.73	5 ± 1	0.3	0.64
2.5	4 ± 1	0.55	0.4	5 ± 1	0.34	0.63	5 ± 2	0.39	0.61
2.0	8 ± 1	0.47	0.47	4 ± 1	0.44	0.56	3 ± 1	0.39	0.61
1.5	7 ± 1	0.71	0.27	4 ± 1	0.63	0.40	3 ± 1	0.46	0.54
1.0	5 ± 2	0.92	0.08	4 ± 1	0.97	0.03	3 ± 1	0.48	0.52
0.7	3 ± 1	0.49	0.51	4 ± 1	0.73	0.27	4 ± 1	0.46	0.54
0.5	4 ± 1	0.35	0.65	4 ± 1	0.89	0.11	4 ± 1	0.53	0.47
0.4	5 ± 1	0.7	0.3	4 ± 1	0.89	0.11	5 ± 1	0.51	0.49
0.3	3 ± 1	0.35	0.65	3 ± 1	0.93	0.07	4 ± 1	0.42	0.58

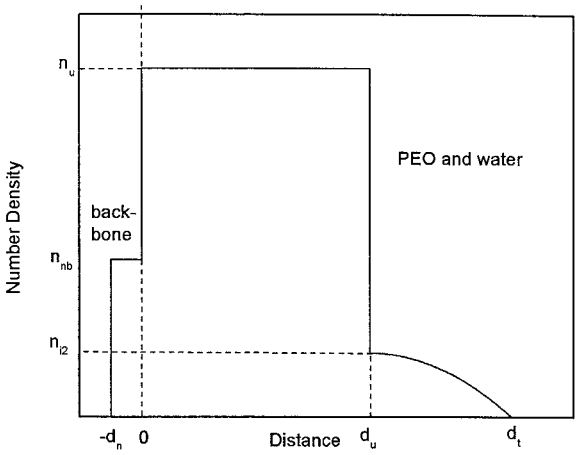

Figure 5. Schematic of model number density distribution profiles indicating the parameters determining the distribution.

used in the expressions below for the number density distribution.

$$-d_n \le z \le 0 \qquad n_{nb}$$

$$0 \le z \le d_u \qquad n_u$$

$$d_u \le z \le d_t \qquad n_p = n_{i2}(1 - (z + d_u)^2/d_t^2)$$

$$z > d_t \qquad n_{eo} = 0$$

where n_{nb} is the number density of norbornene segments in the layer; n_u and n_p are the number densities of ethylene oxide segments immersed in the subphase in the two layers. The latter is described by a parabolic distribution of segments, the parameters of which are given in Figure 5. This parabolic distribution prevails at greater depths below the surface; immediately below the surface the poly(ethylene oxide) grafts form a layer of uniform composition. Typical fits to the reflectometry data for the part deuterated copolymers spread on an nrw subphase are shown in Figure 4.

For all graft copolymers and for all concentrations the polynorbornene layer was of an approximately constant thickness of 5 ± 2 Å. This layer contains a considerable volume fraction of air according to the scattering length density values obtained. The air volume fraction was never less than 0.3, and surprisingly, larger air volume fractions were a feature of the higher surface concentrations (Table 2). Figure 6 shows a selection of the segment density distributions obtained for the n50 graft copolymer at different surface concentrations. The major effect of increasing the surface concentration is to increase the thickness of the PEO uniform layer region (in addition to increasing the number density of ethylene oxide segments). Figure 6 also compares the number density profiles of the n50 and n15 graft copolymers at the highest and lowest spread film surface concentrations. For both concentrations the profiles have the same general features; i.e., the transition to a parabolic distribution starts at a higher number density for the n15 copolymer than the n50 copolymer, and the uniform layer number densities for both copolymers are rather similar to each other at the differing surface concentrations despite the difference in molecular weight of the grafts. The concentration of poly(ethylene oxide) was calculated from the parameters of the distribution using the relation

$$\Gamma_{eo}/\text{mg m}^{-2} = \frac{10^{23} m_{eo}}{N_A}\left(n_u d_u + \frac{4}{3} n_{i2} d_t\right) \qquad (5)$$

where m_{eo} is the molar mass of an ethylene oxide segment and N_A is Avogadro's number. For all surface concentrations of all graft copolymers the concentration profiles calculated from the fitting to the reflectivity data accounted for at least 94% of the actual poly(ethylene oxide) spread, and for the majority of data sets the uniform layer−parabola model accounted for over 96% of the spread poly(ethylene oxide).

Discussion

The organization of this graft copolymer is rather different than that of the polystyrene−poly(ethylene oxide) diblock copolymers discussed by Bisterbosch et al. where an adsorbed layer of PEO was evident at low surface concentrations, a brushlike layer of PEO on top of this adsorbed layer proposed for the higher surface concentrations.[12] Notably, there is no evidence for an adsorbed PEO layer, and moreover the volume fraction of air in the polynorbornene layer increases, albeit with no apparent regularity, as the spread film is compressed; we attempt to rationalize this observation. The double bonds that remain in the backbone introduce some rigidity, and the backbone is somewhat puckered and does not lie completely flat on the surface of the aqueous subphase. Molecular simulations of the ungrafted backbone reveal a tendency for it to adopt a helical organization when compressed at the chain ends.[41] Formation of helical structures would lift more of the molecule from the surface and incorporate a greater volume fraction of air in this backbone layer. Such compression along the backbone may be occurring at the higher surface concentrations where packing restricts gross movement of copolymer molecules. Since the repulsive potential between hydrocarbon backbone and PEO grafts (see below) will increase as the surface

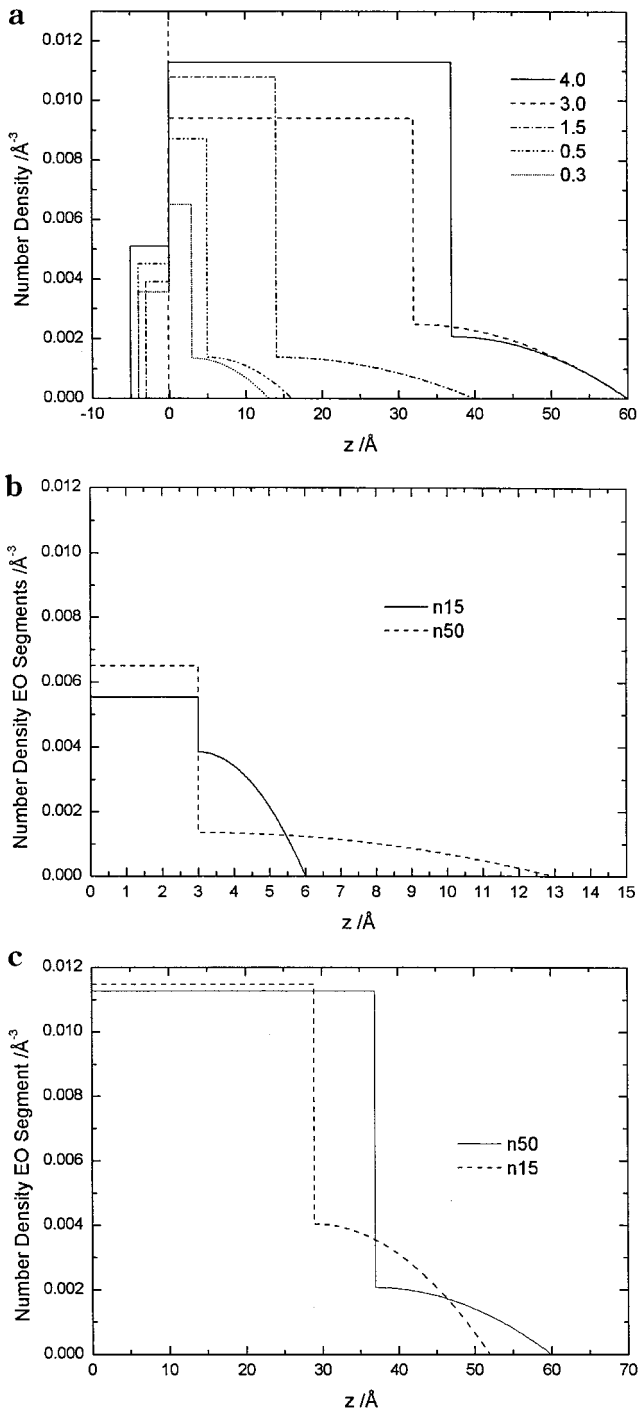

Figure 6. Number density distribution profiles for graft copolymer (a) n50 at differing surface concentrations, (b) n50 and n15 at a surface concentration of 0.3 mg m^{-2}, and (c) n50 and n15 at a surface concentration of 4.0 mg m^{-2}.

concentration increases, a consideration could be that this repulsion causes the norbornene backbone to "lift" from the water surface somewhat. However, since each monomer unit in the backbone has a PEO graft, effectively pinning the backbone to the surface at each monomer unit (unlike diblock amphiphilic copolymers where there is only a single pinning point) this mechanism is not believed to be significant. We remark that the scattering length density of the backbone is low; thus, neutron reflectivity is not very sensitive to small changes in the dimensions and composition of this layer, and this may be the cause of the irregularity in the values of Table 3.

Since aqueous poly(ethylene oxide) homopolymer solutions form a surface excess layer, there is evidently an attractive interaction of the polymer with the air−water interface. Because of the hydrophobic nature of polynorbornene the interaction with the hydrophilic poly(ethylene oxide) is likely to be repulsive. Consequently, spreading a thin film of the graft copolymer at the air−water interface conforms rather closely to the conditions defined by Szleifer in his theoretical analysis of bush layer thickness. There is one major difference: the grafting density of the air−water interface by the PEO grafts may be low on average but remains very high along the direction of the backbone chain for each molecule on the surface. Molecular simulations show that at low surface concentrations the grafts extending in the plane of the interface either side of the backbone and adopting a rather flat configuration at the interface relieve the intramolecular interactions between grafts. At high surface concentrations, interactions between grafts from other copolymer molecules force a stretching of them deeper into the subphase. For comparison with various theories of tethered chains we require values for the number of tethered chains per unit area, i.e., the grafting density σ. On the assumption that all the poly(ethylene oxide) grafts are immersed in the subphase, then

$$\sigma = \frac{50\Gamma_s \times 10^{-3} N_A}{M_c}$$

where M_c is the number-average molecular weight of the copolymer. These grafting densities are normalized for the different radii of gyration of the PEO grafts; i.e., we use σ^* as defined by Szleifer where

$$\sigma^* = \sigma\pi R_g^{\,2}$$

and R_g is the radius of gyration of the graft, values being calculated from relationships provided by Kawaguchi et al.[40] To quantify the layer thickness, we have used the sum of the uniform layer thickness plus the thickness of the parabolic region, i.e., the distance marked as d_t in Figure 5. Other definitions have been used to quantify the layer thickness, e.g., the first moment and the ellipsometric thickness, but all will have the same scaling with σ^*; only the absolute values of the layer thickness differ, depending on the method used to calculate the layer thickness from the composition distribution profile obtained. The uniform layer thickness (d_u), parabolic region thickness ($d_t - d_u$), and the total layer thickness (d_t) of the PEO layer are given for all the surface concentrations investigated for each copolymer in Table 3. The total PEO layer thickness (normalized by graft radius of gyration) dependence on σ^* for all graft copolymers is shown in Figure 7. For the n50 and n25 graft copolymers the data fall on a common curve whereas the n15 data are initially coincidental with data for the other two copolymers, but for values of $\sigma^* = 2$ and above the d_t/R_g values are 1.5−2 times those for the n50 and n25 copolymers. The difference in the values of d_t/R_g for the n15 copolymer is attributed to the higher proportion of cis tactic sequences in the backbone of the polymer molecule. The curves for the n50 and n25 copolymers have the form given by Szleifer (Figure 1b) for low values of the repulsion parameter between the tethered chains and the surface. The dependence of the layer thickness of

Table 3. Uniform, Parabolic, and Total PEO Layer Thickness for All Graft Copolymers at the Air−Water Interface

	n15			n25			n50		
Γ_s/mg m^{-2}	d_u/Å	$d_t - d_u$/Å	d_t/Å	d_u/Å	$d_t - d_u$/Å	d_t/Å	d_u/Å	$d_t - d_u$/Å	d_t/Å
4	29 ± 2	23 ± 3	52 ± 4	25 ± 1	23 ± 2	48 ± 2	37 ± 2	23 ± 2	60 ± 3
3.5	22 ± 2	30 ± 2	52 ± 2	22 ± 1	24 ± 3	46 ± 2	33 ± 1	29 ± 1	62 ± 1
3	18 ± 3	27 ± 4	45 ± 5	12 ± 2	31 ± 2	43 ± 2	32 ± 1	28 ± 2	60 ± 2
2.5	15 ± 3	25 ± 2	40 ± 4	13 ± 1	30 ± 2	43 ± 2	26 ± 2	30 ± 2	56 ± 3
2	12 ± 2	30 ± 3	42 ± 3	11 ± 1	25 ± 1	36 ± 1	19 ± 1	35 ± 3	54 ± 3
1.5	8 ± 2	28 ± 2	36 ± 2	6 ± 2	24 ± 1	30 ± 2	14 ± 1	26 ± 4	40 ± 5
1	9 ± 1	23 ± 1	32 ± 1	11 ± 1	17 ± 4	28 ± 4	5 ± 1	27 ± 2	32 ± 2
0.7	4 ± 1	13 ± 1	17 ± 1	5 ± 2	17 ± 1	22 ± 2	11 ± 2	19 ± 4	30 ± 4
0.5	4 ± 1	7 ± 1	11 ± 1	5 ± 1	12 ± 1	17 ± 1	5 ± 1	11 ± 3	16 ± 3
0.4	3 ± 1	7 ± 1	10 ± 1	5 ± 1	7 ± 1	12 ± 1	5 ± 1	13 ± 5	18 ± 5
0.3	3 ± 1	3 ± 1	6 ± 1	5 ± 1	4 ± 3	9 ± 3	5 ± 1	10 ± 3	15 ± 3

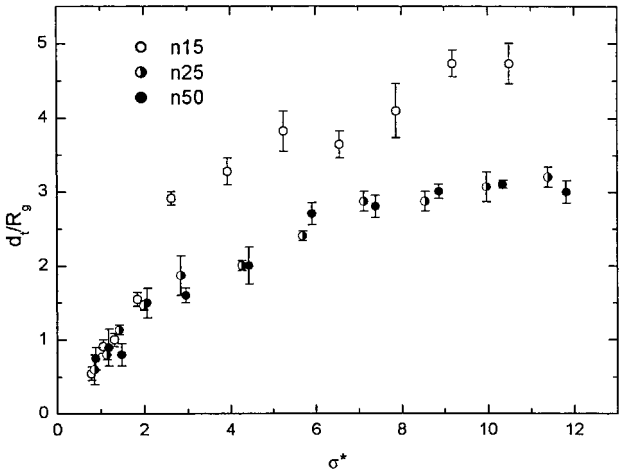

Figure 7. Total thickness, d_t, of poly(ethylene oxide) layer as a function of σ^*.

Table 4. Scaling Exponents for the Relation between h/R_g and σ^*

copolymer	$0 < \sigma^* \leq 3$	$3 \leq \sigma^* \leq 12$
n50	0.71	0.3
n25	0.94	0.4_8
n15	1.4	0.4

the n15 copolymer on σ^* has a greater resemblance to the curve obtained for increased repulsion between the surface layer and the tethered chain. For the n25 and n50 graft copolymers the extension of the PEO grafts at the highest surface coverage is rather modest, being only 3 times the radius of gyration. By contrast, the n15 copolymer approaches ca. 5 times the radius of gyration, close to the value predicted by Szleifer[35] for finite values of the repulsive interaction parameter, χ_{rep}. Double-logarithmic plots have been used to obtain the scaling exponents α in the relation

$$d_t/R_g \sim \sigma^{*\alpha}$$

Two values of α were obtained for each spread copolymer film: one value pertains to the range $0 \leq \sigma^* \leq 3$, the second value being for the range $3 \leq \sigma^* \leq 12$. Table 4 gives the values of α obtained from linear least-squares fits. Only for the n50 copolymer in the highest range of σ^* values does the exponent have the value of 0.3 as predicted by both the scaling and analytical self-consistent-field theories of brushlike layers. Double-logarithmic plots of the predictions of the dependence of layer thickness on surface concentration from single-chain mean-field theory (Figure 1b) give values of the exponent that depends on both the surface concentration and the strength of the repulsive interaction between the anchor and buoy component of the copolymer. For $\chi_{rep} = 0$, in the low surface concentration region, the exponent α has a value of ca. 2; this decreases to 0.5 in the higher surface concentration region. For large χ_{rep}, the exponents for the same two surface concentration regimes are 2.9 and 0.2, respectively. Evidently, the exponents reported in table for $0 < \sigma^* \leq 3$ are considerably smaller than the theoretical predictions; however, for $3 \leq \sigma^* \leq 12$ the observed exponents fall between the limiting values predicted by the theory of Szleifer. This suggests that a repulsive interaction exists between the solvated PEO grafts and the polynorbornene backbone covering the aqueous surface; i.e., χ_{rep} has a finite value. In concert with the earlier plots for the surface pressure, Figure 7 shows no evidence of a region of σ^* where there is no variation in the layer thickness followed by an abrupt increase when the first-order transition takes place. If the individual thicknesses of the uniform layer, d_u, and the parabolic layer, $(d_t - d_u)$, are normalized by R_g and plotted as a function of σ^*, rather different behavior is observed for these two lengths (Figure 8). For all three copolymers $(d_t - d_u)/R_g$ increases regularly from the lowest surface concentration until $\sigma^* \simeq 6-8$ where after it either has a constant value or decreases somewhat. By contrast, the parameter associated with the uniform layer, d_u/R_g, appears to be roughly constant for $\sigma^* \leq 2$ and then increasing at an approximately constant rate as σ^* increases. It appears that the first-order phase transition is confined to those segments that make up the uniform layer of poly(ethylene oxide) in the subphase. Although the change in composition of the copolymers with respect to each other is small, the relative proportion of polynorbornene backbone to poly(ethylene oxide) graft is higher for the n15 copolymer than for the n50. Consequently, if the growth of the uniform layer thickness is due to repulsions between the grafts and the polynorbornene covered aqueous surface, we anticipate that the value of σ^* where this increasing thickness becomes evident should be lowest in the n15 copolymer and highest in the n50 copolymer. The data are somewhat scattered for the n15 copolymer, but the value of σ^* where d_u/R_g begins to increase is marginally lower than that for the n25 copolymer where $\sigma^* \sim 2$ seems to be the critical value, and for the n50 copolymer, this value is ∼3.

Conclusions

A series of graft copolymers with a polynorbornene backbone in which every repeat unit carried a poly(ethylene oxide) graft have been prepared with similar backbone degree of polymerization but with a range of three different degrees of polymerization for the poly(ethylene oxide) grafts. These graft copolymers form

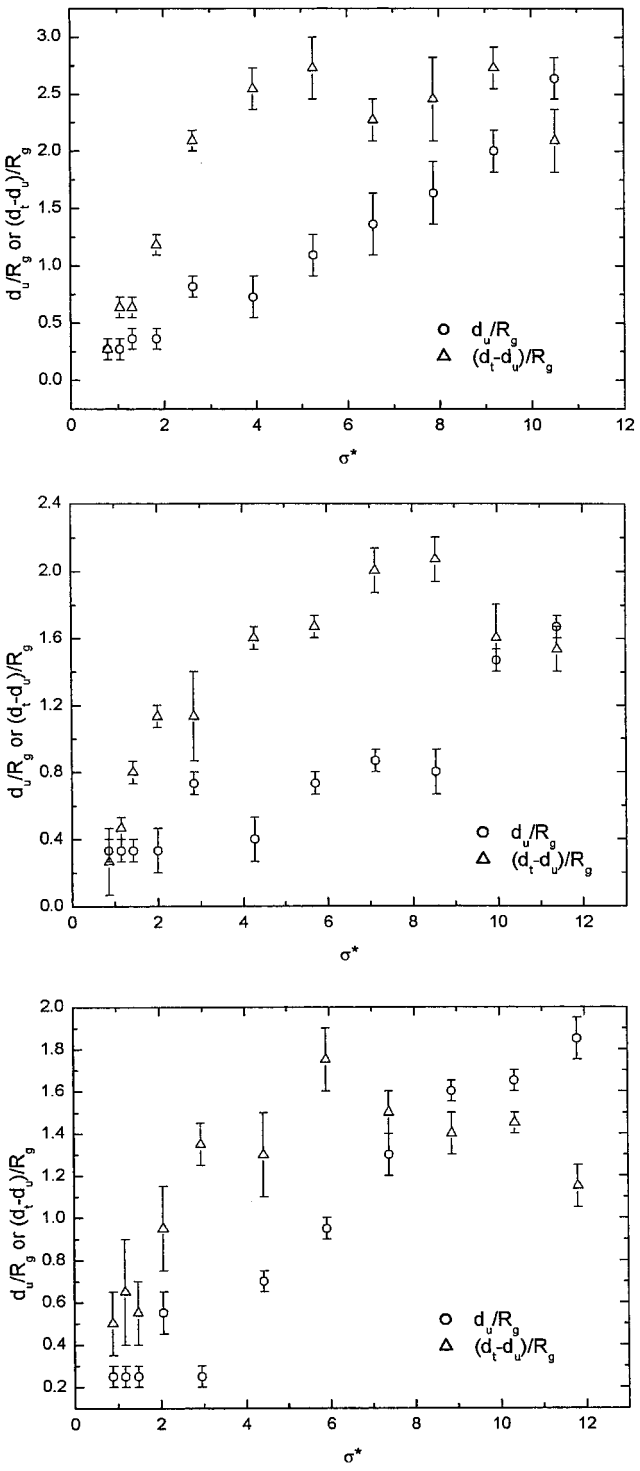

Figure 8. Uniform layer, d_u, and parabolic region, $(d_t - d_u)$, thickness for each graft copolymer as a function of σ^*: (a) n15, (b) n25, (c) n50.

stable films when spread at the air−water interface, and the influence of the molecular weight of the grafts is seen in the surface pressure isotherms. Neutron reflectometry data are best fitted by a model that has a layer of polynorbornene resting on the aqueous subphase with the poly(ethylene oxide) grafts essentially completely immersed in the subphase. The poly(ethylene oxide) distribution is described by a uniform layer immediately below the water surface with a parabolic "tail" at the distances furthest from the surface. As the surface concentration of the graft copolymer increases, the poly(ethylene oxide) layer thickness increases in a manner that has been predicted by single-chain mean-field theory where the increase in the dimensions is attributed to increased repulsions between the grafts and the backbone on the surface as the surface becomes increasingly covered by the hydrocarbon backbone. The dependence of the overall layer thickness does not exhibit the scaling exponent of 0.33 predicted by theory in any concentration range, but the observed exponents do fall in the range of values predicted by single-chain mean-field theory for high surface concentrations. There is no evidence in either the surface pressure isotherm or the total layer thickness data for the first-order phase transition that theory predicts. However, the thickness of the uniform layer region remains constant for a limited range of surface concentrations before a distinct increase in thickness at a constant rate becomes evident. The thickness of the region where the composition decay is parabolic begins to increase immediately when the surface concentration is increased but approaches an asymptotic value (or even decreases slightly) at the higher surface concentrations where the uniform layer thickness is still increasing.

Acknowledgment. We thank the EPSRC for the financial support of the research program of which this work forms part and a maintenance grant to A.F.M. CCLRC is thanked for the provision of neutron reflectometry instrumentation. We thank Dr. M. Wilson of Durham University for his assistance in the molecular simulations and Professor I Szleifer of Purdue University for making the data in Figure 1 available.

References and Notes

(1) Alexander, S. *J. Phys. (Paris)* **1977**, *38*, 977−981.
(2) de Gennes, P. G. *Macromolecules* **1980**, *13*, 1069−1075.
(3) Dolan, A. K.; Edwards, S. F. *Proc R. Soc London, Ser. A* **1975**, *343*, 427−442.
(4) Milner, S. T.; Witten, T. A.; Cates, M. E. *Macromolecules* **1988**, *21*, 2610−2619.
(5) Milner, S. T.; Witten, T. A.; Cates, M. E. *Macromolecules* **1989**, *22*, 853−861.
(6) Aubouy, M.; Guiselin, O.; Raphael, E. *Macromolecules* **1996**, *29*, 7261−7268.
(7) Napper, D. H. *Polymeric Stabilisation of Colloid Dispersions*; Academic Press: New York, 1983.
(8) Amiji, M.; Park, K. *J. Biomater. Sci., Polym. Ed.* **1993**, *4*, 217−234.
(9) Gast, A. P. *Langmuir* **1996**, *12*, 4060−4067.
(10) Jones, R. A. L.; Norton, L. J.; Shull, K. R.; Kramer, E. J.; Felcher, G. P.; Karim, A.; Fetters, L. J. *Macromolecules* **1992**, *25*, 2359−2368.
(11) Auroy, P.; Auvray, L.; Leger, L. *Macromolecules* **1991**, *24*, 2523−2528.
(12) Bisterbosch, H. D.; de Haan, V. O.; de Graaf, A. W.; Mellema, M.; Leermakers, F. A. M.; Cohen-Stuart, M. A.; van Well, A. A. *Langmuir* **1995**, *11*, 4467−4473.
(13) Henderson, J. A.; Richards, R. W.; Penfold, J.; Thomas, R. K.; Lu, J. R. *Macromolecules* **1993**, *26*, 4591−4600.
(14) Henderson, J. A.; Richards, R. W.; Penfold, J.; Thomas, R. K. *Macromolecules* **1993**, *26*, 65−75.
(15) Peace, S. K.; Richards, R. W.; Taylor, M. R.; Webster, J. R. P.; Williams, N. *Macromolecules* **1998**, *31*, 1261−1268.
(16) Ou-Yang, D.; Gao, Z. *J Phys II* **1991**, *1*, 1375−1385.
(17) Auvray, L.; de Gennes, P. G. *Europhys. Lett.* **1986**, *2*, 647−650.
(18) Patel, S. S.; Tirrell, M. *Annu. Rev. Phys. Chem.* **1989**, *40*, 597−635.
(19) Penfold, J.; Thomas, R. K. *J. Phys: Condens. Matter* **1990**, *2*, 1369−1412.
(20) Jones, R. A. L.; Richards, R. W. *Polymers at Surfaces and Interfaces*; Cambridge University Press: Cambridge, 1999.

(21) Styrkas, D. A.; Thomas, R. K.; Adib, Z. A.; Davis, F.; Hodge, P.; Liu, X. H. *Macromolecules* **1994**, *27*, 5504−5510.
(22) Miller, A. F.; Richards, R. W.; Webster, J. R. P. *Macromolecules* **2000**, *33*, 7618.
(23) Gissing, S. K.; Richards, R. W.; Rochford, B. R. *Colloids Surf. A: Physicochem. Eng. Aspects* **1994**, *86*, 171−183.
(24) Kent, M. S.; Majewski, J.; Smith, G. S.; Lee, L. T.; Satija, S. *J. Chem. Phys.* **1999**, *110*, 3553−3565.
(25) Lee, L. T.; Kent, M. S. *Phys. Rev. Lett.* **1997**, *79*, 2899−2902.
(26) Lee, L. T.; Factor, B. J.; Kent, M. S.; Rondelez, F. *Physica B* **1996**, *221*, 320−324.
(27) Lee, L. T.; Factor, B. J.; Rondelez, F.; Kent, M. S. *Faraday Discuss.* **1994**, 139−147.
(28) Kent, M. S.; Factor, B. J.; Satija, S.; Gallagher, P.; Smith, G. S. *Macromolecules* **1996**, *29*, 2843−2849.
(29) Kent, M. S.; Lee, L. T.; Factor, B. J.; Rondelez, F.; Smith, G. S. *J. Chem. Phys.* **1995**, *103*, 2320−2342.
(30) Kent, M. S.; Lee, L. T.; Farnoux, B.; Rondelez, F. *Macromolecules* **1992**, *25*, 6240−6247.
(31) Factor, B. J.; Lee, L. T.; Kent, M. S.; Rondelez, F. *Phys. Rev. E* **1993**, *48*, R2354−R2357.
(32) Ligoure, C. *J. Phys. II* **1993**, *3*, 1607−1617.
(33) Li, T.; Park, K. *Comput. Theor. Polym. Sci.* **2001**, *11*, 133−142.
(34) Szleifer, I.; Carignano, M. A. *Adv. Chem. Phys.* **1996**, *XCIV*, 165−260.
(35) Szleifer, I. *Europhys. Lett.* **1998**, *44*, 721−727.
(36) Szleifer, I.; Carignano, M. A. *Macromol. Rapid Commun.* **2000**, *21*, 423−448.
(37) Carignano, M. A.; Szleifer, I. *Macromolecules* **1995**, *28*, 3197−3204.
(38) Vilanove, R.; Rondelez, F. *Phys. Rev. Lett.* **1980**, *45*, 1502−1505.
(39) Daoud, M.; Jannink, G. *J. Phys. (Paris)* **1975**, *37*, 973−979.
(40) Kawaguchi, M. *Prog. Polym. Sci.* **1993**, *18*, 341−376.
(41) Miller, A. F.; Richards, R. W. Unpublished results.

MA010873T